Laser-induced fluorescence spectra of the HgZn excimer: Transitions involving the $E0^-$, $A1$, $A0^-$, and $B0^-$ states

E. Hegazi, J. Supronowicz, J. B. Atkinson, and L. Krause
Department of Physics, University of Windsor, Windsor, Ontario, Canada N9B 3P4
and Ontario Laser and Lightwave Research Centre, Windsor, Ontario, Canada N9B 3P4
(Received 20 September 1989)

Excitation and fluorescence spectra arising from bound-bound transitions between the $E0^-$ and the $A1$, $A0^-$, and $B0^-$ states of the HgZn excimer were investigated using pump-and-probe methods of laser spectroscopy. Several previously unknown bands were recorded, interpreted, and analyzed, yielding vibrational constants, relative energies, and relative internuclear separations for the various states.

I. INTRODUCTION

We have recently described and analyzed an extensive system of laser-induced fluorescence (LIF) and excitation spectra associated with the $E1$ (Hg $6\,^1S$ + Zn $4\,^1P$) and $F1$ (Hg $6\,^1S$ + Zn $5\,^3S$) states of the HgZn excimer.[1] The spectra were correlated with a potential-energy (PE) diagram that was obtained from a theoretical calculation[1] based on Hund's case-(c) coupling which, although still preliminary, supersedes a previous PE diagram based on Hund's case-(a) coupling.[2] In the course of further experiments, we discovered additional band systems which were clearly associated with transitions between the states indicated on the PE diagram.[1] A partial PE diagram drawn according to Hund's case-(c) coupling and containing the $A1$, $A0^-$, $A0^+$, $B0^-$, and $E0^-$ states is sketched in Fig. 1. As may be seen by inspection of the case-(a) and case-(c) PE diagrams,[1] the $^3\Sigma$ and $^3\Pi$ states, correlated with the Hg($6\,^1S$) and Zn($4\,^3P$) atomic states, split into six components: three with $\Omega=0$ ($A0^-, A0^+, B0^-$), two with $\Omega=1$ ($A1, B1$), and one with $\Omega=2$ ($A2$). Of these, the $A0^-$, $B0^-$, and $A2$ are expected to be metastable since their decay to the $\Omega=0^+$ ($^1\Sigma^+$) ground state is forbidden by selection rules. The relative ordering of these and the more highly excited Ω states, and the positions of the PE minima, are influenced by the various curve crossings and anticrossings.[1]

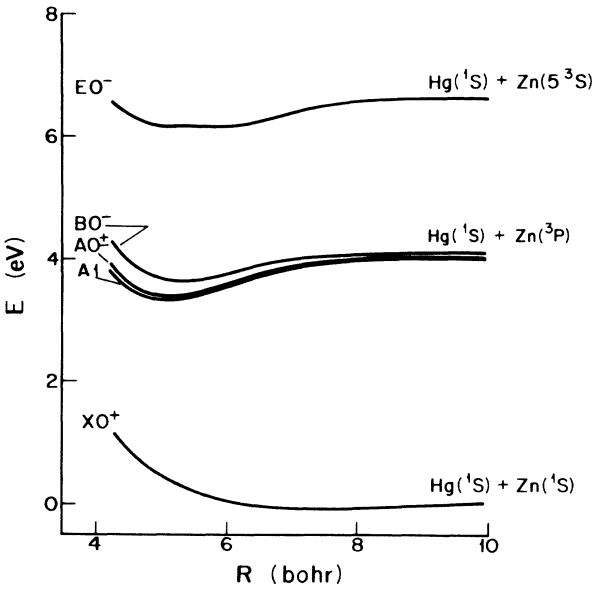

FIG. 1. A partial PE diagram showing the $A1$, $A0^-$, $A0^+$, $B0^-$, and $E0^-$ states. 0^+, 0^-, and 1 are the values of Ω in Hund's case-(c) coupling. $A0^\pm$ denotes unresolved $A0^+$ and $A0^-$ PE curves. A complete set of PE curves may be found in Ref. 1.

In the present investigation we recorded two excitation spectra and four bound-bound fluorescence spectra which are assigned to various transitions involving the $E0^-$, $A1$, $A0^-$, and $B0^-$ spin-orbit states. Analysis of the bands yielded the respective vibrational constants and provided estimates of the relative positions of the minima on the PE diagram.

II. EXPERIMENTAL DETAILS

A. Description of the apparatus

The apparatus used in this investigation has been described in detail elsewhere.[3] The second harmonic of the output from a Q-switched Nd:YAG laser (where YAG denotes yttrium aluminum garnet) was used to pump a two-stage, in-house built dye laser which contained a solution of rhodamine 640 in methanol. The dye-laser output at 6152 Å was frequency doubled by a potassium dihydrogen phosphate (KDP) crystal and the resulting 3076-Å radiation which had a linewidth of about 2 cm^{-1} and corresponded to the Zn $4\,^3P_1 \leftarrow 4\,^1S_0$ transition, was focused into a quartz fluorescence cell containing a mixture of Hg and Zn vapors at a temperature of about 840 K. The Hg vapor pressure was approximately 2.2 atm and the Zn pressure about 1 torr. After a 450-ns delay, when the $4\,^3P$ Zn atoms were no longer present in the vapor and the HgZn molecular states were thermalized, the cell was probed with collinear pulses of light from a second dye laser pumped by a N_2 laser. The resulting HgZn molecular fluorescence was observed at right angles to the laser beams, dispersed with a monochromator and detected with a photomultiplier whose output was time resolved with a transient digitizer. The resulting

time spectra were summed in a microcomputer which also controlled the scanning of the monochromator and the probe dye laser.

The cylindrical fluorescence cell had a sidearm protruding downwards whose temperature was controlled separately. The amount of mercury in the cell was such that at temperatures above 660 K all of it was in the vapor phase. The temperature of the sidearm controlling the Zn vapor density was usually kept at about 780 K.

The probe dye laser was tuned using an achromatic quad-prism beam expander[4] and a Littrow-mounted diffraction grating which could be scanned in constant wavelength increments by a computer-controlled stepper motor; the laser produced a linewidth of about 0.3 cm^{-1} and the smallest step corresponded to an increment of $\frac{1}{24}$ Å. A small fraction of the output was directed onto a fast photodiode to generate a trigger signal for the acquisition system. The typical time half-width of both pump and probe pulses was approximately 8 ns.

The fluorescence spectra were resolved with a 0.32-m Jobin-Yvon HR-320 monochromator fitted with an 1800-line/mm holographic grating, and were detected with a cooled RCA 31034A photomultiplier. The monochromator, whose resolution limit was 0.5 Å, was equipped with a computer-controlled stepper motor which scanned it in constant wavelength increments; the finest step corresponded to 0.1 Å. The photomultiplier output was digitized with a Biomation Model 6500 waveform analyzer and the resulting time spectrum was transferred to a Commodore PET 2001 microcomputer in which the spectra resulting from a number of laser pulses were summed and averaged.

B. Experimental procedure

The experiment consisted of two separate but complementary parts: scans of the fluorescence spectra and scans of the excitation spectra. To scan a fluorescence spectrum, the probe laser was tuned to a transition from a vibrational level of a low-lying HgZn state, populated during the pump process, to a vibrational level of a higher-lying state. The resulting fluorescence, emitted as the result of various bound-bound transitions, consisted of several band systems each of which was investigated further using the following procedure. The monochromator was set by the computer to a particular starting wavelength, the photomultiplier output was digitized after each laser pulse and the resulting time spectra produced by a set number (usually 10) of laser pulses were summed and stored in the computer memory location corresponding to the monochromator setting; the computer then advanced the monochromator by a preset wavelength increment and the procedure was repeated until the end of the chosen spectral region was reached, after which the monochromator was reset to the initial setting and the scan was repeated until a satisfactory signal-to-noise ratio was achieved. This signal averaging procedure was successful in bringing out the bound-bound fluorescence bands from the intense and long-persisting background fluorescence in the same wavelength region.[2] The bands contained information about the vibrational structure of the lower states participating in the transitions. Some of the spectra were emitted in transitions between the two electronic states that were involved in the absorption of the probe radiation, with one vibrational component being of the same wavelength as the probe radiation (resonance fluorescence). When deemed appropriate, the probe wavelength was subsequently tuned to a different $v' \leftarrow v''$ transition between the same two electronic states.

During the scans of the excitation spectra, the data-acquisition procedure was similar to that described above, with one significant difference. The monochromator setting was fixed to correspond to vibrational component of a fluorescence band and the probe laser was scanned across the band. In this way we monitored LIF yield in relation to the excitation wavelength. The resulting excitation spectra contain information about the vibrational structure of the absorbing state.

III. RESULTS AND DISCUSSION

The transitions obey the selection rules appropriate to Hund's case-(c) coupling for heteronuclear molecules:[5]

(1) $\Delta\Omega = 0, \pm 1$ ($\Delta J \neq 0$ for $\Omega = 0 \leftrightarrow \Omega = 0$).

(2) For transitions $\Omega = 0 \leftrightarrow \Omega = 0, + \leftrightarrow +, - \leftrightarrow -, - \not\leftrightarrow +$.

During the present investigation we observed several fluorescence and excitation spectra in the blue spectral region, which we attribute to bound-bound transitions between various electronic states. The interpretation and analysis of the spectra have been carried out on the basis of the selection rules and the PE diagram shown in Fig. 1 and in conjunction with numerous additional fluorescence and excitation spectra all of which are consistent with the scheme presented here.[1,6]

A. The fluorescence spectrum in the 4000–4450-Å region

Figure 2 shows a trace of two superimposed fluorescence bands emitted in the bound-bound decay of the $v'=0$ level of the $E0^-$ state to the $A1$ and $A0^-$ states. The $v'=0$ level was excited with the probe laser wavelength 4189 Å corresponding to the $E0^-$, $v'=0 \leftarrow A1$, $v''=2$ transition which could not be observed in fluorescence because of background from scattered laser light, and which is indicated in Fig. 2 with a dashed profile whose estimated intensity was obtained by exciting the same v' level with probe laser light of different wavelength. The $v'=0 \rightarrow v''=0$ components were located at 4122 Å in the $E0^- \rightarrow A1$ band system and at 4236 Å in the $E0^- \rightarrow A0^-$ band system. Accordingly, the energy separation between the $v=0$ levels of the $A1$ and $A0^-$ states was found to be 650 ± 7 cm^{-1}. The distribution of the relative intensities for each band has a single maximum, typical of $v'=0$ emission bands. In both bands the pattern of relative intensities among the vibrational components is similar, with transitions to $v'' > 5$ being too weak to be detected, and this similarity supports the conclusion that the r_e values associated with the state $A1$ and $A0^-$ are almost equal. The spectrum in Fig. 2 includes the atomic Hg 4358 and 4047 Å lines which serve

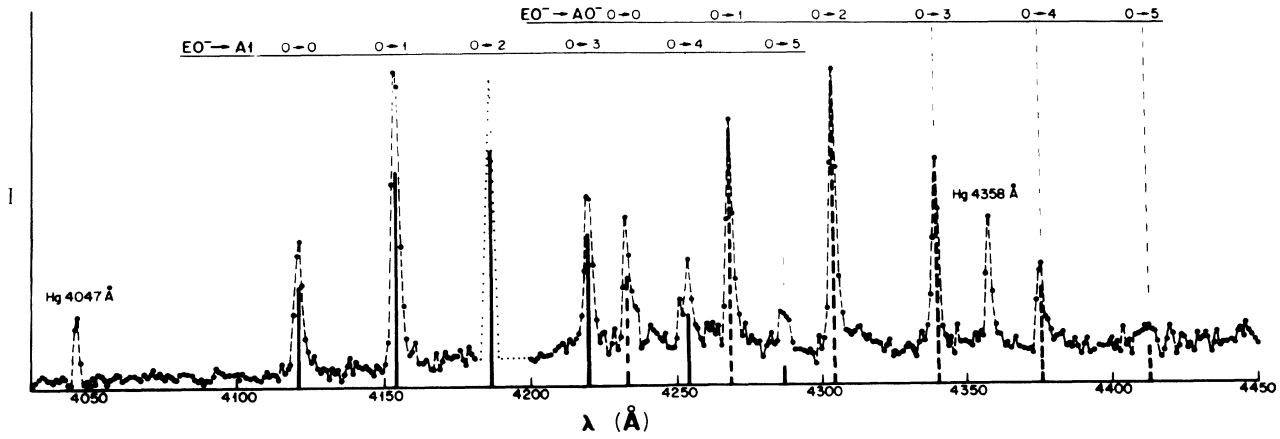

FIG. 2. A trace of two fluorescence bands arising from $E0^- \rightarrow A1$ and $E0^- \rightarrow A0^-$ transitions, showing $v'=0 \rightarrow v''$ assignments. The dashed profile indicates the peak corresponding to the probe wavelength. The vertical bars indicate the vibrational intensities derived from the computer simulation.

as convenient points of reference. The trace also shows the vibrational assignments of the various components.

Probing the system with laser radiation at 4096 Å resulted in the excitation of the $v'=1$ level of the $E0^-$ state from the $v''=0$ level of the $A1$ state and in the emission of the fluorescence spectrum shown in Fig. 3 which contains both $E0^- \rightarrow A1$ and $E0^- \rightarrow A0^-$ bands and also includes the 4047- and 4358-Å Hg lines. We are carrying out further experiments to elucidate the mechanism responsible for the presence of these atomic lines in the spectrum. The relative intensities of the vibrational components indicate that the r_e values for the $A0^-$ and $A1$ states are nearly equal. When the probe laser wavelength was tuned to 4306 Å which excited the $E0^-$, $v'=0 \leftarrow A0^-$, $v''=2$ transition, or to 4208 Å which excited the $E0^-$, $v'=1 \leftarrow A0^-$, $v''=0$ transition, the resulting fluorescence spectra were similar to those shown in Figs. 2 and 3, respectively.

The wavelengths, frequencies, and frequency separations of the vibrational components of the $E0^- \rightarrow A1$ and $E0^- \rightarrow A0^-$ band systems are listed in Tables I and II, respectively. The frequencies were substituted in the standard term equation[5] and subjected to a least-squares analysis which yielded the respective vibrational constants.

B. The fluorescence spectrum in the 4600–4780-Å region

A very intense bound-bound fluorescence band, registered in the 4600–4780-Å region, is attributed to transitions between the vibrational levels of the $E0^-$ state and those of another lower state which is believed to be the $B0^-$ state. A trace of this band, shown in Fig. 4, exhibits a v'' progression which represents the vibrational spacing of the $B0^-$ state. The band was excited with 4189-Å probe radiation which excited the $E0^-$, $v'=0 \leftarrow A1$, $v''=2$ transition. The most intense fluorescence component corresponds to the $E0^-$, $v'=0 \rightarrow B0^-$, $v''=1$ emission at 4676 Å; transitions from $v'=0$ to $v''>4$ were too faint to be detected because of small Franck-Condon (FC) factors and because their small signals were swamped by the intense fluorescence continuum emitted by the long-lived $A0^+$ and $A1$ states, which has a peak at 4750 Å.[2,7] From the wavelength of the $E0^-$,

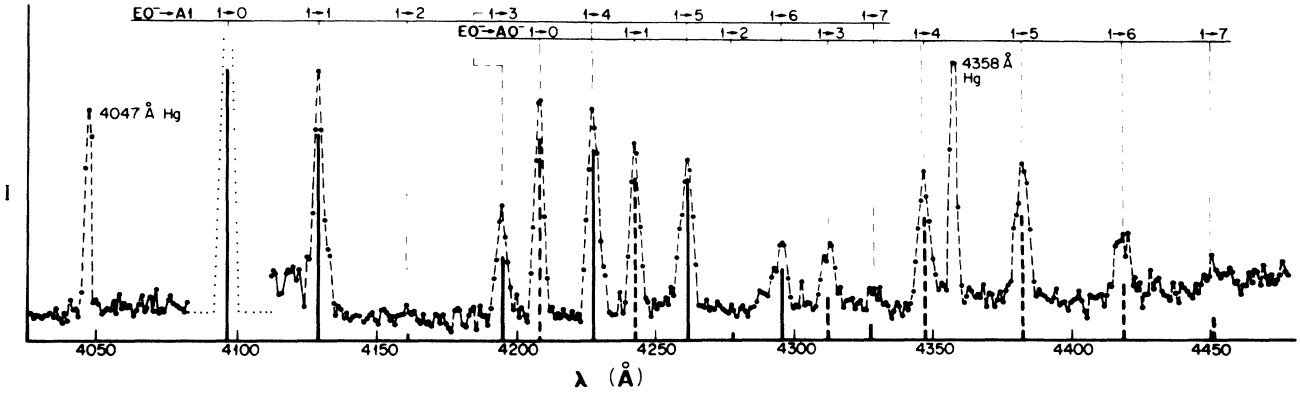

FIG. 3. A trace of two fluorescence bands arising from $E0^- \rightarrow A1$ and $E0^- \rightarrow A0^-$ transitions, showing $v'=1 \rightarrow v''$ assignments. The dotted profile indicates the peak corresponding to the probe wavelength. The vertical bars indicate the intensities derived from the computer simulation.

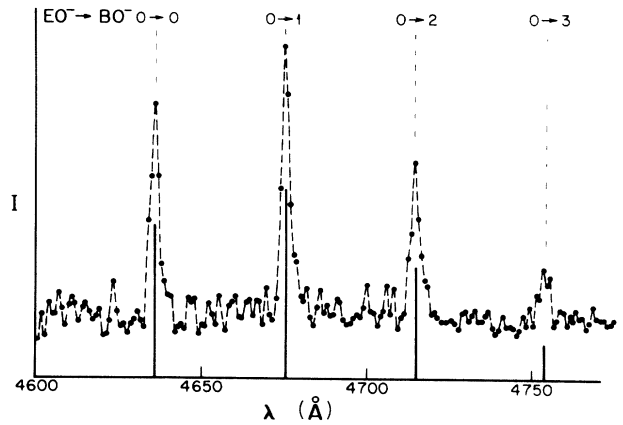

FIG. 4. A trace of the fluorescence band excited with 4189-Å probe radiation and originating from the $E0^-$, $v'=0\rightarrow B0^-$, v'' transitions, showing $v'\rightarrow v''$ assignments. The vertical bars indicate the intensities derived from the computer simulation.

$v'=0\rightarrow B0^-$, $v''=0$ component which we found to be 4637 Å, we concluded that the $A1$-$B0^-$ energy separation was 2690±7 cm^{-1}. Figure 5 shows the trace of the fluorescence band resulting from the decay of the $E0^-$, $v'=1$ state to various $B0^-$, v'' states. The $v'=1$ level was excited with 4096-Å probe radiation which induced the $E0^-$, $v'=1\leftarrow A1$, $v''=0$ transition. The relative intensities of the vibrational components are determined mainly by the FC factors; again, transitions with $v'=1\rightarrow v''>5$ were too faint to be detected. The wavelengths, frequencies, and frequency separations of the components in the $E0^-\rightarrow B0^-$ band are listed in Table III. Fluorescence spectra similar to those shown in Figs. 4 and 5 were produced when the probe laser was tuned to 4306 Å which excited the $E0^-$, $v'=0\leftarrow A0^-$, $v'=2$ transition, or to 4208 Å which excited the $E0^-$, $v'=1\leftarrow A0^-$, $v''=0$ transition, respectively. When substituted in the standard term equation and subjected to least-squares analysis, they yielded the vibrational constants for the $B0^-$ state.

TABLE I. Vibrational components of the $E0^-\rightarrow A1$ fluorescence band. The measured λ are in air and $\tilde{\nu}$ are stated in vacuo.

$v'\rightarrow v''$	λ (Å)	$\tilde{\nu}$ (cm^{-1})	$\Delta\tilde{\nu}$ (cm^{-1})
0→0	4122±1	24 253±5	
			198
0→1	4156±1	24 055±5	
			190
0→2	4189±1	23 865±5	
			192
0→3	4223±1	23 673±5	
			183
0→4	4256±1	23 490±5	
			186
0→5	4290±2	23 304±10	
1→0	4096±1	24 407±5	
			189
1→1	4128±1	24 218±5	
			192
1→2	4161±1	24 026±5	
			189
1→3	4194±1	23 837±5	
			192
1→4	4228±2	23 645±8	
			183
1→5	4261±1	23 462±5	
			186
1→6	4295±2	23 276±10	
			182
1→7	4329±3	23 094±15	

C. The excitation spectrum in the 4180–4130-Å region

Since the $E0^-$ state was found to emit fluorescence bands in its decay to the $A1$, $A0^-$, and $B0^-$ states, it should be expected that the $E0^-\leftarrow A1$ and $E0^-\leftarrow A0^-$ excitation spectra should have the same profiles when monitored at any wavelength corresponding to a vibrational component in the $E0^-\rightarrow A1$, $E0^-\rightarrow A0^-$ (4000–4450 Å) or $E0^-\rightarrow B0^-$ (4600–4780 Å) fluorescence bands. This we found to be the case; at the same time we also found that we were not able to produce an $E0^-\leftarrow B0^-$ excitation spectrum. We believe that the $A0^-$, $A1$, and $B0^-$ states are in thermal equilibrium and, since the population of the $B0^-$ is only 1% of the $A1$ population, the absorption is too small to be observed. Figure 6 shows an excitation spectrum in the 4180–4310-Å region, monitored at 4676 Å, a fluorescence component which corresponds to the $E0^-$, $v'=0\rightarrow B0^-$,

TABLE II. Vibrational components of the $E0^-\rightarrow A0^-$ fluorescence band. The measured λ are in air and $\tilde{\nu}$ are in vacuo.

$v'\rightarrow v''$	λ (Å)	$\tilde{\nu}$ (cm^{-1})	$\Delta\tilde{\nu}$ (cm^{-1})
0→0	4236±1	23 601±5	
			194
0→1	4271±1	23 407±5	
			190
0→2	4306±1	23 217±5	
			193
0→3	4342±1	23 024±5	
			184
0→4	4377±2	22 840±10	
1→0	4208±1	23 758±5	
			191
1→1	4242±1	23 567±5	
			193
1→2	4277±2	23 374±10	
			189
1→3	4312±2	23 185±10	
			187
1→4	4347±1	22 998±5	
			189
1→5	4383±2	22 809±10	
			186
1→6	4419±3	22 623±15	
			183
1→7	4455±4	22 440±20	

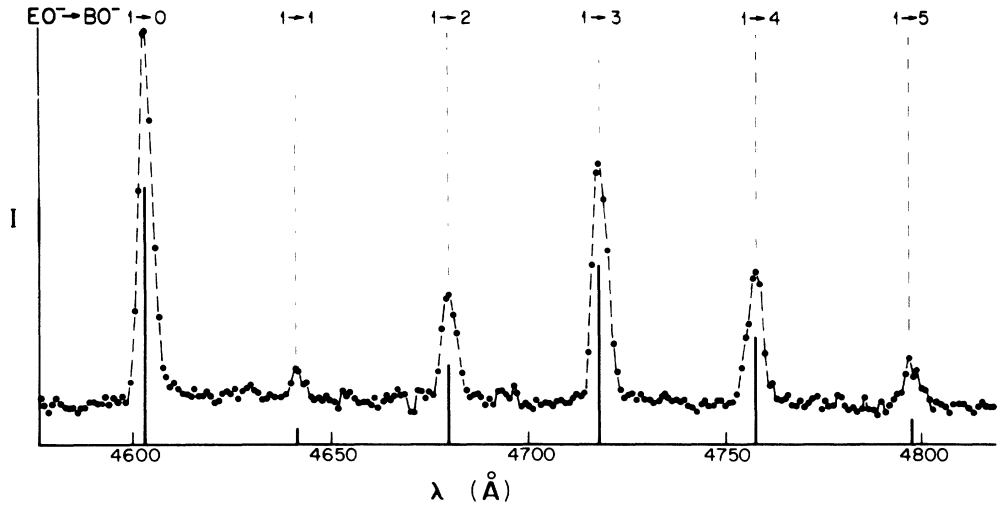

FIG. 5. A trace of the fluorescence band excited with 4296-Å probe radiation and originating from the $E0^-$, $v'=1\rightarrow B0^-$, v'' transitions, showing $v'\rightarrow v''$ assignments. The vertical bars indicate the intensities derived from the computer simulation.

$v''=1$ transition; virtually identical profiles were recorded when the excitation spectrum was monitored on the $E0^-$, $v'=0\rightarrow A1$, $v''=1$ or the $E0^-$, $v'=0\rightarrow A0^-$, $v''=1$ component of the fluorescence band. This consistency confirms our assignments of the various bound-bound transitions and the associated bands, and reinforces our conclusions concerning the relative positioning of the $A1$, $A0^-$, $B0^-$, and $E0^-$ states on the energy scale.

The trace shown in Fig. 6 also resembles the central segment of the fluorescence spectrum shown in Fig. 2. This is not surprising since we believe both spectra to represent v'' progressions of the $A1$ and $A0^-$ states. Another example of an excitation spectrum is shown in Fig. 7; there the $E0^-$, $v'=1$ state was excited from various $A1$, v'' and $A0^-$, v'' states and the spectrum was monitored at 4603 Å, a component corresponding to the $E0^-$, $v'=1\rightarrow B0^-$, $v''=0$ transition. An identical excitation spectrum was recorded when the fluoresecence was monitored on the $E0^-$, $v'=1\rightarrow A1$, $v''=0$ or the $E0^-$, $v'=1\rightarrow A0^-$, $v''=0$ component. The structure of this spectrum closely resembles that shown in Fig. 3 which is a trace of the corresponding fluorescence spectrum.

TABLE III. Vibrational components of the $E0^-\rightarrow B0^-$ fluorescence band. The measured λ are in air and $\tilde{\nu}$ are in vacuo.

$v'\rightarrow v''$	λ (Å)	$\tilde{\nu}$ (cm^{-1})	$\Delta\tilde{\nu}$ (cm^{-1})
0→0	4637±1	21 560±5	
			180
0→1	4676±1	21 380±5	
			177
0→2	4715±1	21 203±5	
			174
0→3	4754±2	21 029±10	
1→0	4603±1	21 719±5	
			183
1→1	4642±1	21 536±5	
			174
1→2	4680±1	21 362±5	
			177
1→3	4719±1	21 185±5	
			174
1→4	4758±1	21 011±5	
			170
1→5	4797±2	20 841±10	

D. Interpretation of spectral-intensity profiles

The intensities of the vibrational components in Figs. 2–7 exhibit variations which arise not only from the

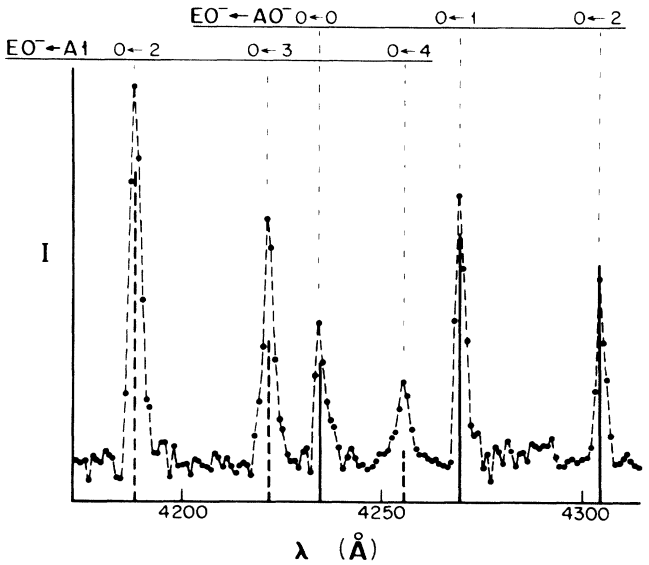

FIG. 6. A trace of the $E0^-$, $v'=0\leftarrow A1$, v'' and $E0^-$, $v'=0\leftarrow A0^-$, v'' excitation bands, monitored at 4676 Å. The vertical bars indicate the intensities derived from the computer simulation.

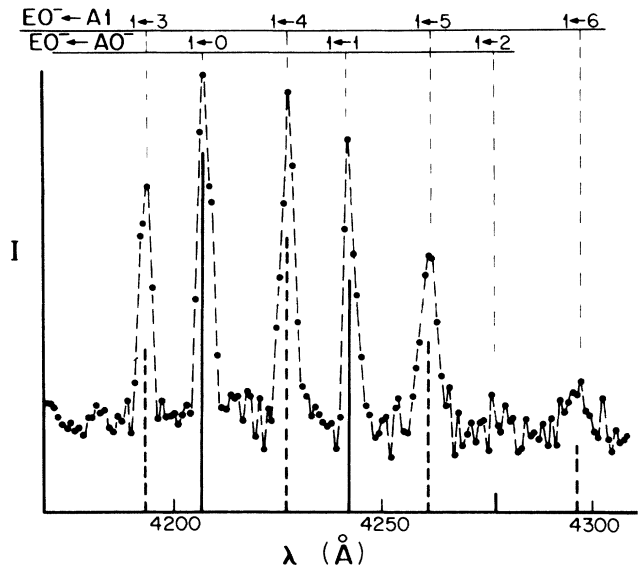

FIG. 7. A trace of the $E0^-$, $v'=1\leftarrow A1$, v'' and $E0^-$, $v'=1\leftarrow A0^-$, v'' excitation bands, monitored at 4719 Å. The vertical bars indicate the intensities derived from the computer simulation.

wavelength dependence of the dye-laser intensity, response of the detection system, and temperature conditions in the cell, but also from FC factors. To account for the intensity distributions in the vibronic bands, we carried out a computer simulation of the bands, a procedure which also yielded additional information about the various HgZn states.

The procedure involved the calculation of FC factors for the various vibronic transitions, assuming the Morse potential[8] for both upper and lower states (which we believe to be a good approximation near the PE minimum) and the experimentally determined values ω_e and $\omega_e x_e$. The wave functions of both states were calculated analytically[8] and the vibrational overlap integral $\int \psi''_v(r)\psi'_v(r)dr$ was determined by numerical integration. The integral was then squared to obtain the FC factors which, in the case of the fluorescence bands, were further corrected for the ν^3 dependence of the emission intensity and the spectral response of the spectrometer. These corrections were quite important for the success of the simulation procedure. For use in excitation bands, the FC factors were corrected for the Boltzmann distribution and normalized to the relative probe laser output power. The Boltzmann correction for a $v'\leftarrow v''$ component has the form $\exp(-\Delta E/kT)$ where $\Delta E=G(v'')-G(v''=0)$, and $kT=570$ cm^{-1} corresponded to the experimental conditions. We assumed a constant (independent of r) transition moment for the transitions between the electronic states since all the spectra involved v' or v'' progressions in which one or the other vibrational level was $v=0$ or $v=1$. In the excited states observed here ω is in the range 150–195 cm^{-1} and the reduced mass of HgZn is 49 a.u. The classically accessible region of r, within which the transitions would be expected to take place, extends over a range of less than 0.25 Å and we believe that over such a small region of r the transition moments may be assumed constant to a reasonable approximation.

To calculate the intensity distribution within a particular progression, we varied Δr_e the difference between the equilibrium internuclear separations in the upper and lower electronic states, to obtain a band profile which was the best match of the experimental trace. The simulated intensity profiles of the various bands are shown by vertical bars drawn under the corresponding experimentally registered vibrational peaks in Figs. 2–7 where it may be seen that there is a very good detailed agreement between the observed and the calculated intensity distributions. The Δr_e values yielded by the calculations are listed in Table IV together with the other molecular constants obtained from the fluorescence and excitation spectra.

IV. SUMMARY AND CONCLUSIONS

Several fluorescence and excitation spectra arising from bound-bound transitions between the $E0^-$ and the $A1$, $A0^-$, and $B0^-$ states of the HgZn excimer were recorded and analyzed. The analysis yielded vibrational constants for the various states as well as their relative energies and equilibrium internuclear separations r_e; the data are summarized in Table IV.

TABLE IV. Molecular constants obtained from the fluorescence and excitation spectra.

HgZn state	ΔE (cm^{-1})[a]	ω_e (cm^{-1})	$\omega_e x_e$ (cm^{-1})	Δr_e (Å)[e]
$A1$	0	195±3[b]	0.9±0.2[b]	0.004±0.003[b]
$A0^-$	650±7[b] 600[d]	194±3[b] 194±6[c]	0.7±0.2[b]	0
$B0^-$	2690±7[b] 2900[d]	182±2[b]	1.0±0.2[b]	0.033±0.003[b]
$E0^-$	24 250±5[b] 22 990[d]	158±4[b]	0.5±0.3	0.138±0.002[b]

[a]ΔE is the energy of the $v=0$ level relative to the $A1$, $v=0$ state.
[b]This investigation.
[c]Reference 1.
[d]Estimated from the PE diagram.
[e]$\Delta r_e=r_e-r_e(A0^-)$.

The experimentally recorded fluorescence and excitation bands arising from the transitions between the states shown in Fig. 1, considered in conjunction with the selection rules and with numerous additional spectra,[1,6] provide a basis for the identification of the states. The assignments shown in Tables I–IV are consistent with the observed transitions. The identification of $E0^-$ as the upper state participating in the transitions is corroborated by the absence of any bound-continuum fluorescence spectrum, since the decay of the $E0^-$ state to the $X0^+$ ground state is forbidden. Transitions between the $E0^-$ and the $A0^+$ and $A2$ states are also forbidden by the selection rules and thus the $A0^-$ and $A1$ states are the only possible lower states that can participate in the transitions in the 4100–4450-Å region. In the 4600–4780-Å region, only transitions to the $B0^-$ and $B1$ states are allowed. We believe the $B0^-$ state to be the more likely lower state.

The excitation spectra reported here and in previous publications[1,7] all support the conclusion that the lowest bound states of HgZn are in thermal equilibrium and that only the $A1$, $A0^-$, and $A0^+$ states have sufficient population to be observed in the excitation spectra. The experimentally determined energy separations between the various states agree quite well with the values predicted by the PE diagram, and the scheme shown in Fig. 1 provides a sensible interpretation of the observed transitions between the states $A1$, $A0^-$, $B0^-$, and $E0^-$.

ACKNOWLEDGMENTS

This research was supported by the Canadian Department of National Defence through the Unsolicited Proposals Program, and by the Natural Sciences and Engineering Research Council of Canada.

[1]E. Hegazi, J. Supronowicz, J. B. Atkinson, and L. Krause, Phys. Rev. A **40**, 6293 (1989).
[2]J. Supronowicz, E. Hegazi, G. Chambaud, J. B. Atkinson, W. E. Baylis, and L. Krause, Phys. Rev. A **37**, 295 (1988).
[3]R. J. Niefer, J. Supronowicz, J. B. Atkinson, and L. Krause, Phys. Rev. A **34**, 1137 (1986).
[4]R. J. Niefer and J. B. Atkinson, Opt. Commun. **67**, 139 (1988).
[5]G. Herzberg, *Spectra of Diatomic Molecules* (Van Nostrand, New York, 1950).
[6]E. Hegazi, J. Supronowicz, J. B. Atkinson, and L. Krause, following paper, Phys. Rev. A **42**, 2741 (1990).
[7]J. Supronowicz, E. Hegazi, J. B. Atkinson, and L. Krause, Phys. Rev. A **37**, 3818 (1988); **39**, 4892 (1989).
[8]P. M. Morse, Phys. Rev. **34**, 57 (1929).